Published in final edited form as:

Nature. 2008 November 13; 456(7219): 202–208. doi:10.1038/nature07473.

Deconstructing voltage sensor function and pharmacology in sodium channels

Frank Bosmans[1,2], **Marie-France Martin-Eauclaire**[3], and **Kenton J. Swartz**[1]

[1]Molecular Physiology and Biophysics Section, Porter Neuroscience Research Center, National Institute of Neurological Disorders and Stroke, National Institutes of Health, Bethesda, MD 20892 USA

[2]Laboratory of Toxicology, University of Leuven, 3000 Leuven, Belgium

[3]CNRS UMR 6132, CRN2M, Institut Jean Roche, Université de la Méditerranée, Marseille Cedex 20, France

Abstract

Voltage-activated sodium (Nav) channels are crucial for the generation and propagation of nerve impulses, and as such are amongst the most widely targeted ion channels by toxins and drugs. The four voltage sensors in Nav channels have distinct amino acid sequences, raising fundamental questions about their relative contributions to the function and pharmacology of the channel. Here we use four-fold symmetric voltage-activated potassium (Kv) channels as reporters to examine the contributions of individual Nav channel S3b-S4 paddle motifs to the kinetics of voltage sensor activation and to forming toxin receptors. Our results uncover binding sites for toxins from tarantula and scorpion venom on each of the four paddle motifs in Nav channels and reveal how paddle-specific interactions can be used to reshape Nav channel activity. One paddle motif is unique in that it slows voltage sensor activation and toxins selectively targeting this motif impede Nav channel inactivation. This reporter approach and the principles that emerge will be useful in developing new drugs for treating pain and Nav channelopathies.

Nav channels in nerve and muscle cells open and close, or gate, in response to changes in membrane voltage1. Mutations in Nav channels can cause a variety of inherited disorders, such as epilepsy and myotonia2, 3. Furthermore, Nav channels are strategically positioned within nociceptive signaling pathways, with mutations leading to severe pain disorders4, 5. Although the development of drugs interacting with Nav channels is of widespread medical importance6, progress has been slow because the architecture and gating mechanisms of these ion channels are complex. Their channel-forming α-subunits contain four homologous domains (I-IV), or pseudosubunits, each containing six transmembrane segments (S1-S6) (Fig.1a). The S5-S6 segments collectively form a central pore for Na^+, with the S1-S4

Correspondence and requests for materials should be addressed to K.J.S. (swartzk@ninds.nih.gov). .

Author Information Reprints and permissions information is available at npg.nature.com/reprints. The authors declare no competing financial interests.

Full Methods and any associated references are available in the online version of the paper at www.nature.com/nature.

segments from each domain forming the surrounding voltage sensors1. Each of the four voltage sensors activate in response to changes in voltage, however, those in domains I-III are most important for channel opening, while the one in domain IV is crucial for fast inactivation7-10. Thus, drugs and toxins can interact with multiple regions of Nav channels to influence their activity, with the four voltage sensors representing rich, yet complex targets. The similarity of the four voltage sensors raises the possibility of multiple binding sites, with occupancy of each having distinct effects on gating. Indeed, seven different receptor sites have been proposed for drugs and toxins that interact with Nav channels1, 11, but only a few have been molecularly defined. Here we develop an approach for studying the unique contributions of the four voltage sensors in Nav channels to gating and pharmacology. We identify S3b-S4 paddle motifs that can be transplanted from Nav channels into Kv channels without disrupting function, while transferring sensitivity to classical Nav channel toxins. Our results uncover rich interactions between toxins and multiple Nav channel paddle motifs, and reveal how domain specific interactions can be used to reshape Nav channel activity.

Transferring paddle motifs between Nav and Kv channels

Studies on voltage sensors in Kv channels have identified an S3b-S4 helix-turn-helix motif, the voltage-sensor paddle, which moves at the protein-lipid interface to drive activation of the voltage sensors and opening of the pore12-16. The paddle motif is an important pharmacological target in Kv channels, as tarantula toxins that partition into membranes interact with this region to inhibit channel opening12, 17-24. Our initial goal was to determine whether paddle motifs can be defined in Nav channels and whether they fulfill similar functions. Since paddle motifs are portable modules that are interchangeable between Kv channels and voltage-sensing proteins12, we wondered whether distinct paddle motifs in each of the four voltage sensors of Nav channels could be transplanted into a homotetrameric Kv channel to study them in isolation (Fig. 1a). We initially transplanted the paddle motifs from rNav1.2a and rNav1.4 into the Kv2.1 channel. Although the sequences of these Nav and Kv channel paddle motifs vary substantially, constructs containing specific S3b-S4 regions of Nav channels result in fully functional channels that display robust voltage-activated potassium currents (Fig.1b,c, Supplementary Fig.1,2a and Supplementary Table 1). Functional chimaeras were also obtained by transplanting the paddle motif from rNav1.4 into Kv1.3 and Shaker Kv channels (Supplementary Fig.1,2b,c, Supplementary Table 2), demonstrating that paddle motifs of Nav and Kv channels are generally interchangeable.

Transferring toxin sensitivity between Nav and Kv channels

We next asked whether transplanting isolated paddle motifs from Nav channels into Kv channels faithfully transfers sensitivity to toxins, in which case the Kv channel could be used as a reporter for investigating interactions between toxins and individual Nav channel paddle motifs. Tarantula toxins related to those targeting paddle motifs in Kv channels12, 17-22, 24 (Supplementary Fig.1d) inhibit Nav channels by modifying gating25-27, however,

Supplementary Information is linked to the online version of the paper at www.nature.com/nature.

their presumed receptors within the four voltage sensors of Nav channels have yet to be defined. We focused on three tarantula toxins, PaurTx3, ProTx-I and ProTx-II25-27 and tested whether they interact with the Kv2.1 channels containing each of the four paddle motifs from rNav1.2a. Remarkably, sensitivity to these toxins can be transferred to Kv2.1 along with specific Nav channel paddle motifs (Fig.2a). PaurTx3 has the simplest profile of the three, as this toxin only inhibits the Kv channel containing the paddle motif from domain II (Fig.2a, Supplementary Fig.3a and Supplementary Table 3). In contrast, ProTx-I and ProTx-II interact with multiple paddle motifs from rNav1.2a. ProTx-I binds to Kv2.1 containing the paddle motifs from domain II or IV, whereas ProTx-II interacts with those from domains I, II or IV. (ProTx-I also inhibits Kv2.126, however, the lack of toxin sensitivity for the domain I and III chimaeras support interaction of the toxin with paddle motifs.) Although it is not straightforward to directly correlate the apparent affinities of Kv channel paddle chimaeras and Nav channels because the paddles are identical in Kv channels and different in Nav channels, the concentration-dependence for toxin inhibition of the two channel types are remarkably similar (Supplementary Fig.4a,b; Supplementary Table 3). These results show that tarantula toxins often interact with multiple paddle motifs in Nav channels, a scenario that would be difficult to detect using conventional approaches27, 28.

Landmark studies on scorpion venom have established the presence of two classes of toxins, the α- and β-scorpion toxins, that interact with the voltage sensors in domains IV and II of Nav channels, respectively1, 29-33. In the conventional view, these toxins interact with solvent-exposed extracellular loops between S3 and S4 to stabilize the voltage sensors in specific states8, 31, 34. Whether these toxins interact with the larger S3b-S4 paddle motif, or can target voltage sensors in domains other than II and IV, is unknown. To explore these possibilities we tested whether we could make Kv2.1 sensitive to the classical α- and β-scorpion toxins. As in the case of tarantula toxins, transfer of Nav channel paddle motifs into Kv2.1 renders the channel sensitive to the α-scorpion toxin AaHII, however, in this instance only the paddle motif from domain IV can transfer toxin sensitivity (Fig.2a; Supplementary Fig.3a). Although the apparent affinity of AaHII for the domain IV chimaera is considerably less than for rNav1.2a (Supplementary Fig.4d; Supplementary Table 3), mutations within S4 can increase the apparent affinity by over 10-fold (Fig.3d,4c; Supplementary Fig.4d). These results suggest that α-scorpion toxins interact with the paddle motif from domain IV, but the modest affinity of the paddle chimaera leaves open the possibility that other regions of Nav channels contribute to the toxin receptor35.

We also examined whether sensitivity to the β-scorpion toxin TsVII could be transferred with Nav channel paddle motifs. In contrast to AaHII, transfer of the paddle motifs from domains II, III or IV from rNav1.2a renders the Kv channel sensitive to TsVII (Fig.2a; Supplementary Fig.3a), revealing that β-scorpion toxins can interact with multiple Nav channel paddle motifs. This result is surprising because studies on rNav1.4 suggest that TsVII only binds to the voltage sensor in domain II36, 37. To explore whether scorpion toxin interactions vary between Nav channel subtypes, we tested the sensitivity of the rNav1.4 paddle chimaeras to TsVII. In contrast to what is observed with the rNav1.2a paddles, TsVII can interact selectively with the domain II paddle from rNav1.4 (Fig.2b; Supplementary Fig.3b). Although the apparent affinities of TsVII for the rNav1.2a paddle

chimaeras are significantly lower than the rNav1.2a channel, the rNav1.4 domain II paddle chimaera is comparable (Supplementary Fig.4c, Supplementary Table 3). An interesting feature of TsVII is that the β-scorpion toxin stabilizes a closed state in the paddle chimaeras (Fig.2), whereas the toxin stabilizes the open state of rNav1.2a (Fig.4b) and rNav1.437 channels. β-scorpion toxins can also stabilize a closed state in certain Nav channels32, indicating that open state stabilization is not always observed. One explanation is that toxin binding to the paddle intrinsically stabilizes a closed state, but in certain Nav channels the toxin can stabilize an open state when it also interact with other regions32, 33. Taken together, these data suggest that both tarantula and scorpion toxins interact with paddle motifs, that multiple paddle motifs can be targeted by individual toxins, and that these interactions can differ between Nav channel subtypes.

Critical residues in the toxin-paddle interaction

To further explore the extent to which toxins interact with S3b-S4 paddle motifs, and to identify mutants for testing whether these toxin-paddle interactions actually occur in Nav channels, we mutated each residue in the transferred paddle regions and measured changes in toxin affinity (Fig.3; Supplementary Fig.4 and Supplementary Tables 4-7). One striking feature of the data is that mutations distributed throughout the S3b-S4 paddle motifs cause dramatic perturbations in the apparent affinity for both tarantula and scorpion toxins, suggesting that these toxins target the larger paddle motif. Many of the most influential mutations are of hydrophobic residues, but mutations of polar residues such as Glu residues in S3b and Arg residues in S4 also have pronounced effects. The present mutagenesis of the domain IV paddle motif correctly identify several mutants previously shown to weaken α-scorpion toxin affinity in Nav channels31, but reveal a larger number of influential mutations, many of which have more pronounced effects on toxin affinity. This highlights an advantage of the reporter approach, which allows individual toxin-paddle interactions to be studied in isolation; toxins can interact with up to four different paddle motifs in Nav channels and the effects of mutations in any one of those can be quite subtle because the others remain unaltered.

Another striking feature of these paddle scans is that mutations perturbing toxin-paddle interactions are rather unique for each toxin-paddle pair. For example, both ProTx-I and ProTx-II interact with the paddle motif from domain II, however, the mutants that weaken toxin affinity only partially overlap. In addition, the mutagenesis results for ProTx-II interacting with paddle motifs from domains I, II and IV identify many influential mutations that differ between the three paddles. This comparison suggests that toxin-paddle interactions do not obey a general lock- and-key mechanism, but that the interfaces vary considerably.

Validating toxin-paddle interactions in rNav1.2a

To validate that the toxin-paddle interactions identified here actually occur in Nav channels, we reconstituted the most influential paddle mutants into rNav1.2a and measured changes in toxin affinity. For tarantula toxins, we examined mutations influencing ProTx-II affinity since this toxin interacts with three of the four Nav channel paddle motifs. Mutations within

the paddle motifs of domains I, II and IV weaken the interaction of ProTx-II with rNav1.2 (Fig.4a), suggesting that the toxin interacts with all three paddle motifs in the Nav channel. The mutations tend to have smaller effects in the Nav channel when compared to the paddle chimaeras (compare Fig.4a with Fig.3a,b,d), which makes sense because the mutations in the Nav channel alter only one of three targeted paddle motifs, whereas in the Kv channel chimaera they alter all four. For the β-scorpion toxin TsVII, we examined mutations within the paddle motif of domain III and found that they diminish the hyperpolarizing shift produced by moderate toxin concentrations (Fig.4b), confirming that the toxin interacts with domain III (in addition to its canonical interaction with domain II). Finally, in the case of the α-scorpion toxin AaHII, we reconstituted a gain-of-function mutation into rNav1.2a and observed that the mutation also increases the apparent affinity of the toxin in the Nav channel (Fig.4c). These results demonstrate that the toxin-paddle interactions uncovered using the reporter approach actually occur in Nav channels.

Unique character of the domain IV paddle motif

The differential coupling of the four voltage sensors in Nav channels to opening and inactivation8, 10, 38-40 is accompanied by differences in the kinetics of voltage sensor activation, with the voltage sensor of domain IV moving slower than the other three10. Given that the paddle motif resides in a relatively unconstrained environment in contact with the surrounding lipid membrane, and that it is the region of the voltage sensor that flexes in response to changes in voltage12-16, 41, we wondered whether the paddle motif itself might be responsible for these kinetic differences. To explore this possibility we measured the kinetics of activation (opening) and deactivation (closing) of the four rNav1.2a paddle chimaeras in Kv2.1 in response to membrane depolarization and repolarization, respectively (Fig.5). At most voltages, the time constants obtained by fitting single exponential functions to current relaxations are notably slower for the domain IV paddle chimaera compared to the other chimaeras and to Kv2.1. This difference is not unique to chimaeras between the rNav1.2a and Kv2.1 channel, but is even more pronounced when transplanting paddle motifs from rNav1.4 into Kv2.1, Kv1.3 or Shaker Kv channels (Supplementary Fig.2). These results demonstrate that the paddle motif in domain IV of Nav channels determines the slower movement of this voltage sensor in response to changes in membrane voltage.

Shaping Nav channel activity with domain-selective interactions

A particularly intriguing outcome of looking at toxin-paddle interactions in isolation is that patterns emerge between the domains targeted and the effects of the toxin on Nav channel activity. Inspection of the profiles for toxin-paddle interactions (Fig.2) reveals that by targeting paddle motifs in domains I, II or III, the overall effect of a toxin is to influence opening of Nav channels, irrespective of whether domain IV is also targeted. The tarantula toxins PaurTx3, ProTx-I, ProTx-II, as well as the β-scorpion toxin TsVII, are examples of this relationship. In contrast, the requirements for influencing inactivation are more stringent; to do so a toxin needs to selectively target the paddle motif in domain IV, as is the case with the α-scorpion toxin AaHII. To test whether this pattern is generally applicable across different toxin families, we searched for a tarantula toxin that selectively interacts with the paddle motif in domain IV and asked whether it influences inactivation. Using our

reporter constructs, we screened various tarantula toxins, including VSTx142, GxTx-1E43, HaTx18 and SGTx144, all of which interact with paddle motifs in Kv channels12, 17-21, 24, 44 and are related in sequence to the Nav channel toxins already studied (Supplementary Fig.1d). VSTx1 (10 μM) and GxTx-1E (500 nM) are inactive against the Nav paddle chimaeras (not shown), whereas both HaTx and SGTx1 exhibit robust effects (Fig.6a). HaTx interacts with paddle motifs from domains I, II and IV, similar to ProTx-II, whereas SGTx1 interacts selectively with the domain IV paddle chimaera, the profile we sought to find. When tested against rNav1.2a, HaTx exhibits robust inhibitory effects, similar to ProTx-II, without significantly altering inactivation (Fig.6b). In contrast, SGTx1 does not inhibit rNav1.2a or alter channel opening, but dramatically reduces the extent of inactivation (Fig. 6c), behaving as an α-scorpion toxin. These results suggest that for a toxin to influence inactivation, it must selectively interact with the paddle motif in domain IV; any additional interactions with the other paddles will alter channel opening.

Discussion

Our results with isolating Nav channel paddle motifs using Kv channels as reporters have three fundamental implications for the function and pharmacology of Nav channels. First, they reveal that paddle motifs can determine the kinetics of voltage sensor activation. For Nav channels to function properly, inactivation must proceed more slowly than opening, a property that has been attributed to slower activation of the voltage sensor in domain IV1, 8, 10, 38, 45. Our results show that the paddle motif in domain IV is unique because it systematically slows activation of any voltage sensor into which it is incorporated (Fig.5; Supplementary Fig.2). The paddle motif resides in a relatively flexible environment and moves in contact with the surrounding lipid membrane12-16, 41, raising the intriguing possibility that interactions of the domain IV paddle motif with lipids are unique and are responsible for slowing voltage sensor activation. Other aspects of Nav channel function are unlikely to be determined by the paddle motif (e.g. cooperative voltage sensor activation10, 37, 46), but the approaches described here may help to identify them.

Second, our results reveal rich interactions of tarantula and scorpion toxins with paddle motifs and establish a number of principles for toxin-paddle interactions in Nav channels where the four paddle motifs are not equivalent. Although α- and β-scorpion toxins are known to interact with domains IV and II, respectively31, 32, the present results demonstrate that each of the paddle motifs are targeted by toxins (Fig.2). In fact, multiple paddle motifs are often targeted by a toxin. Even the β-scorpion toxins can interact with other domains in addition to the canonical interaction with domain II. One unexpected finding is that the profiles of toxin-paddle interactions can differ between subtypes of Nav channels, suggesting that such profiles may be a way of distinguishing Nav channels. Our mutagenesis results with the four paddle motifs in rNav1.2a also show that the pattern of mutants altering toxin affinity is specific for each toxin-paddle pair (Fig.3). The most influential mutants can vary considerably for one toxin interacting with different paddles, or for two related toxins interacting with a single paddle motif.

Finally, the profiles of toxin-paddle interactions that emerge from our studies reveal an important relationship between the effect of a toxin on Nav channel activity and domain-

specific interactions. Alterations in channel opening can be achieved with molecules that interact with any of the first three paddle motifs in Nav channels without regard for whether domain IV is also targeted (e.g. HaTx, ProTx-II, TsVII), whereas influencing inactivation requires that a molecule interact exclusively with the paddle in domain IV (e.g. SGTX1, AaHII). These domain-specific interactions have important implications for designing drugs to reshape Nav channel activity. Channelopathies like idiopathic ventricular fibrillation47 and Long QT syndrome type-348 are associated with accelerated Nav channel inactivation, which could be restored by selectively targeting the domain IV paddle motif. In contrast, the hyperpolarization of Nav channel opening seen in disorders like generalized epilepsy with febrile seizures type 249 and hyperkalaemic periodic paralysis50 could be managed with drugs targeting any paddle motif within the first three domains. Our reporter approach for identifying toxins that specifically target the paddle motif in domain IV (Fig.6) provides a conceptual example for identifying drugs that interact with specific paddle motifs in Nav channels.

METHODS SUMMARY

Channel constructs were expressed in Xenopus oocytes21 and studied using two-electrode voltage-clamp recording techniques. For Kv channel experiments, the external recording solution contained: 50mM KCl, 50mM NaCl, 5mM HEPES, 1mM $MgCl_2$ and 0.3mM $CaCl_2$, pH 7.6 with NaOH. KCl was replaced by RbCl for Shaker experiments. For Nav channel experiments, the external recording solution contained 96mM NaCl, 2mM KCl, 5mM HEPES, 1mM $MgCl_2$ and 1.8mM $CaCl_2$, pH 7.6 with NaOH.

Voltage-activation relationships were obtained by measuring tail currents for Kv channels or steady-state currents and calculating conductance for Nav channels, and a single Boltzmann function was fitted to the data. Occupancy of closed or resting channels by toxins was examined using negative holding voltages where open probability was low, and the fraction of unbound channels (Fu) was estimated using depolarizations that are too weak to open toxin-bound channels, as described previously17-21, 24, 44. The apparent equilibrium dissociation constant (K_d) for toxin interaction with Kv channel constructs was calculated assuming four independent toxin-binding sites per channel, with single occupancy being sufficient to inhibit opening in response to weak depolarizations (See Full Methods, Supplementary Fig. 4, 5c and Supplementary Table 3 for information on K_d measurements.).

Acknowledgements

We thank J.W. Kyle, D.A. Hanck and A.L. Goldin for the rNav1.2a, rNav1.4 and β_1 clones, C. Deutsch for Kv1.3, M.M. Smith for GxTx-1E, K.M. Blumenthal and J.B. Herrington for ProTx-II, L.D. Possani for a sample of Ts1 (or TsVII), the NINDS DNA sequencing facility for DNA sequencing, and the NINDS protein sequencing facility for mass spectrometry and peptide sequencing. We thank AbdulRasheed A. Alabi for helping with Kv and Nav channel alignments and Tsg-Hui Chang for assistance with Nav channel mutants. We also thank AbdulRasheed A. Alabi, Miguel Holmgren, Mark Mayer, Mirela Milescu, Joe Mindell, Andrew Plested, Shai Silberberg and members of the Swartz laboratory for helpful discussions. This work was supported by the Intramural Research Program of the NINDS, NIH and by a NIH-FWO postdoctoral fellowship to F.B.

Appendix

FULL METHODS

Channel and chimaera constructs

Chimaeras and point mutations were generated using sequential polymerase chain reactions (PCR) with Kv2.1Δ719, 51, Kv1.352, Shaker53, rNav1.2a (neuronal type) 54 or rNav1.4 (muscle type)55 as templates. The Kv2.1Δ7 construct contains seven point mutations in the outer vestibule19, rendering the channel sensitive to agitoxin-2, a pore-blocking toxin from scorpion venom56. The Shaker construct contains a deletion of residues 6 to 46 to remove inactivation57. The DNA sequence of all constructs and mutants was confirmed by automated DNA sequencing and cRNA was synthesized using T7/SP6 polymerase (mMessage mMachine kit, Ambion) after linearizing the DNA with appropriate restriction enzymes.

Spider and scorpion toxin purification

PaurTx325 was purified from the venom of *Phrixotrichus* auratus (Spider Pharm) using a new two-step HPLC protocol (Supplementary Fig.5a). Identity and purity were determined with mass spectrometry and automated peptide sequencing. Hanatoxin was purified from *Grammostola spatulata* venom (Spider Pharm) as described previously58. SGTx1 and VSTx1 were synthesized using solid-phase chemical methods, folded *in vitro* and purified as described previously44, 59. AaHII from *Androctonus australis* hector venom (animals collected near Tozeur, Tunisia), and TsVII from *Tityus serrulatus* venom (generous gift from Prof. C. Diniz) were purified as described previously60, 61. Synthetic ProTx-I was acquired from Peptides International (USA). ProTx-II was generously provided by K.M. Blumenthal (SUNY, Buffalo) and J.B. Herrington (Merck Research Labs, Rahway, NJ). GxTx-1E was generously provided by M.M. Smith (Merck Research Labs, Rahway, NJ). The plant alkaloid veratridine (VTD; Sigma, USA) is used as a negative control in Fig.2 since the binding site of this lipid-soluble compound is thought to consist of the S6 transmembrane segments62. Toxins were kept at -20 °C. Before experiments, toxin aliquots were dissolved in appropriate solutions containing 0.1% BSA (or 1% BSA in the case of TsVII).

Two-electrode voltage-clamp recording from Xenopus oocytes

Channel constructs were expressed in Xenopus oocytes21 and studied following 1-2 days incubation after cRNA injection (incubated at 17 °C in 96mM NaCl, 2mM KCl, 5mM HEPES, 1mM $MgCl_2$ and 1.8mM $CaCl_2$, 50μg/ml gentamycin, pH 7.6 with NaOH) using two-electrode voltage-clamp recording techniques (OC-725C, Warner Instruments) with a 150μl recording chamber. Data were filtered at 1 kHz and digitized at 10 kHz using pClamp software (Axon). Microelectrode resistances were 0.1-1MΩ when filled with 3M KCl. For most Kv channel experiments, the external recording solution contained: 50mM KCl, 50mM NaCl, 5mM HEPES, 1mM $MgCl_2$ and 0.3mM $CaCl_2$, pH 7.6 with NaOH. KCl was replaced by RbCl for Shaker experiments. For Nav channel experiments, the external recording solution contained 96mM NaCl, 2mM KCl, 5mM HEPES, 1mM $MgCl_2$ and 1.8mM $CaCl_2$, pH 7.6 with NaOH. For Nav channel experiments, oocytes were co-injected with the β_1

subunit in a 1:5 molar ratio. All experiments were performed at room temperature (~22 °C). Leak and background conductances, identified by blocking the channel with agitoxin-2, have been subtracted for all of the Kv channel currents shown21. Tetrodotoxin subtraction (TTX) or an online P/-4 prepulse protocol was used to isolate Nav channel currents.

Analysis of channel activity and toxin-channel interactions

Voltage-activation relationships were obtained by measuring tail currents for Kv channels or steady-state currents and calculating conductance for Nav channels, and a single Boltzmann function was fitted to the data according to: $I/I_{max} = (1 + e^{-zF(V - V_{1/2})/RT})^{-1}$ where I/I_{max} is the normalized tail-current amplitude, z is the equivalent charge, $V_{1/2}$ is the half-activation voltage, F is Faraday's constant, R is the gas constant and T is temperature in Kelvin.

Occupancy of closed or resting channels by toxins was examined using negative holding voltages where open probability was low, and the fraction of unbound channels (Fu) was estimated using depolarizations that are too weak to open toxin-bound channels, as described previously17-21, 24, 44. After addition of the toxin to the recording chamber, the equilibration between the toxin and the channel was monitored using weak depolarizations elicited at 5-10s intervals. For all channels, we recorded voltage-activation relationships in the absence and presence of different concentrations of toxin. The ratio of currents (I/I_0) recorded in the presence (I) and absence (I_0) of toxin was calculated for various strength depolarizations, typically -70 mV to +10 mV. The value of I/I_0 measured in the plateau phase at voltages where toxin-bound channels do not open was taken as Fu (Supplementary Fig.5b,c). The apparent equilibrium dissociation constant (K_d) for Kv channels was calculated according to $K_d = ((1/(1 - Fu^{1/4})) - 1)[Toxin]$ assuming four independent toxin-binding sites per channel, with single occupancy being sufficient to inhibit opening in response to weak depolarizations. For all chimaeras and mutants, voltage protocols were adjusted appropriately so that the plateau phase in the I/I_0-voltage relationship was well defined. Example traces showing the inhibitory activity of tarantula toxins were taken for relatively weak depolarizations within the plateau phase for that particular channel construct. Off-line data analysis was performed using Clampfit (Axon), Origin 7.5 (Originlab) and Microsoft Solver (Microsoft Excel).

References

51. Frech GC, VanDongen AM, Schuster G, Brown AM, Joho RH. A novel potassium channel with delayed rectifier properties isolated from rat brain by expression cloning. Nature. 1989; 340:642–5. [PubMed: 2770868]

52. Stuhmer W, et al. Molecular basis of functional diversity of voltage-gated potassium channels in mammalian brain. Embo J. 1989; 8:3235–44. [PubMed: 2555158]

53. Tempel BL, Papazian DM, Schwarz TL, Jan YN, Jan LY. Sequence of a probable potassium channel component encoded at Shaker locus of Drosophila. Science. 1987; 237:770–5. [PubMed: 2441471]

54. Auld VJ, et al. A rat brain Na+ channel alpha subunit with novel gating properties. Neuron. 1988; 1:449–61. [PubMed: 2856097]

55. Trimmer JS, et al. Primary structure and functional expression of a mammalian skeletal muscle sodium channel. Neuron. 1989; 3:33–49. [PubMed: 2559760]

56. Garcia ML, Garcia-Calvo M, Hidalgo P, Lee A, MacKinnon R. Purification and characterization of three inhibitors of voltage-dependent K+ channels from Leiurus quinquestriatus var. hebraeus venom. Biochemistry. 1994; 33:6834–9. [PubMed: 8204618]

57. Hoshi T, Zagotta WN, Aldrich RW. Biophysical and molecular mechanisms of Shaker potassium channel inactivation. Science. 1990; 250:533–8. [PubMed: 2122519]

58. Swartz KJ, MacKinnon R. An inhibitor of the Kv2.1 potassium channel isolated from the venom of a Chilean tarantula. Neuron. 1995; 15:941–9. [PubMed: 7576642]

59. Jung HJ, et al. Solution structure and lipid membrane partitioning of VSTx1, an inhibitor of the KvAP potassium channel. Biochemistry. 2005; 44:6015–23. [PubMed: 15835890]

60. Ceard B, De Lima ME, Bougis PE, Martin-Eauclaire MF. Purification of the main beta-toxin from Tityus serrulatus scorpion venom using high-performance liquid chromatography. Toxicon. 1992; 30:105–10. [PubMed: 1595074]

61. Martin MF, Rochat H, Marchot P, Bougis PE. Use of high performance liquid chromatography to demonstrate quantitative variation in components of venom from the scorpion Androctonus australis Hector. Toxicon. 1987; 25:569–73. [PubMed: 3617091]

62. Wang GK, Quan C, Seaver M, Wang SY. Modification of wild-type and batrachotoxin-resistant muscle mu1 Na+ channels by veratridine. Pflugers Arch. 2000; 439:705–13. [PubMed: 10784344]

References

1. Catterall WA. From ionic currents to molecular mechanisms: the structure and function of voltage-gated sodium channels. Neuron. 2000; 26:13–25. [PubMed: 10798388]

2. Cannon SC. Pathomechanisms in Channelopathies of Skeletal Muscle and Brain. Annu Rev Neurosci. 2006

3. George AL Jr. Inherited disorders of voltage-gated sodium channels. J Clin Invest. 2005; 115:1990–9. [PubMed: 16075039]

4. Cox JJ, et al. An SCN9A channelopathy causes congenital inability to experience pain. Nature. 2006; 444:894–8. [PubMed: 17167479]

5. Fertleman CR, et al. SCN9A mutations in paroxysmal extreme pain disorder: allelic variants underlie distinct channel defects and phenotypes. Neuron. 2006; 52:767–74. [PubMed: 17145499]

6. Kaczorowski GJ, McManus OB, Priest BT, Garcia ML. Ion channels as drug targets: the next GPCRs. J Gen Physiol. 2008; 131:399–405. [PubMed: 18411331]

7. Horn R, Ding S, Gruber HJ. Immobilizing the moving parts of voltage-gated ion channels. J Gen Physiol. 2000; 116:461–76. [PubMed: 10962021]

8. Sheets MF, Kyle JW, Kallen RG, Hanck DA. The Na channel voltage sensor associated with inactivation is localized to the external charged residues of domain IV, S4. Biophys J. 1999; 77:747–57. [PubMed: 10423423]

9. Yang N, Horn R. Evidence for voltage-dependent S4 movement in sodium channels. Neuron. 1995; 15:213–8. [PubMed: 7619524]

10. Chanda B, Bezanilla F. Tracking voltage-dependent conformational changes in skeletal muscle sodium channel during activation. J Gen Physiol. 2002; 120:629–45. [PubMed: 12407076]

11. Catterall WA, et al. Voltage-gated ion channels and gating modifier toxins. Toxicon. 2007; 49:124–41. [PubMed: 17239913]

12. Alabi AA, Bahamonde MI, Jung HJ, Kim JI, Swartz KJ. Portability of paddle motif function and pharmacology in voltage sensors. Nature. 2007; 450:370–5. [PubMed: 18004375]

13. Chakrapani S, Cuello LG, Cortes DM, Perozo E. Structural dynamics of an isolated voltage-sensor domain in a lipid bilayer. Structure. 2008; 16:398–409. [PubMed: 18334215]

14. Jiang Y, et al. X-ray structure of a voltage-dependent K+ channel. Nature. 2003; 423:33–41. [PubMed: 12721618]

15. Jiang Y, Ruta V, Chen J, Lee A, MacKinnon R. The principle of gating charge movement in a voltage-dependent K+ channel. Nature. 2003; 423:42–8. [PubMed: 12721619]

16. Ruta V, Chen J, MacKinnon R. Calibrated measurement of gating-charge arginine displacement in the KvAP voltage-dependent K+ channel. Cell. 2005; 123:463–75. [PubMed: 16269337]

17. Swartz KJ, MacKinnon R. Mapping the receptor site for hanatoxin, a gating modifier of voltage-dependent K+ channels. Neuron. 1997; 18:675–82. [PubMed: 9136775]
18. Swartz KJ, MacKinnon R. Hanatoxin modifies the gating of a voltage-dependent K+ channel through multiple binding sites. Neuron. 1997; 18:665–73. [PubMed: 9136774]
19. Li-Smerin Y, Swartz KJ. Gating modifier toxins reveal a conserved structural motif in voltage-gated Ca2+ and K+ channels. Proc Natl Acad Sci U S A. 1998; 95:8585–9. [PubMed: 9671721]
20. Li-Smerin Y, Swartz KJ. Localization and molecular determinants of the Hanatoxin receptors on the voltage-sensing domains of a K(+) channel. J Gen Physiol. 2000; 115:673–84. [PubMed: 10828242]
21. Lee HC, Wang JM, Swartz KJ. Interaction between extracellular Hanatoxin and the resting conformation of the voltage-sensor paddle in Kv channels. Neuron. 2003; 40:527–36. [PubMed: 14642277]
22. Lee SY, MacKinnon R. A membrane-access mechanism of ion channel inhibition by voltage sensor toxins from spider venom. Nature. 2004; 430:232–5. [PubMed: 15241419]
23. Milescu M, et al. Tarantula toxins interact with voltage sensors within lipid membranes. J Gen Physiol. 2007; 130:497–511. [PubMed: 17938232]
24. Phillips LR, et al. Voltage-sensor activation with a tarantula toxin as cargo. Nature. 2005; 436:857–60. [PubMed: 16094370]
25. Bosmans F, et al. Four novel tarantula toxins as selective modulators of voltage-gated sodium channel subtypes. Mol Pharmacol. 2006; 69:419–29. [PubMed: 16267209]
26. Middleton RE, et al. Two tarantula peptides inhibit activation of multiple sodium channels. Biochemistry. 2002; 41:14734–47. [PubMed: 12475222]
27. Smith JJ, Cummins TR, Alphy S, Blumenthal KM. Molecular interactions of the gating modifier toxin ProTx-II with NaV 1.5: implied existence of a novel toxin binding site coupled to activation. J Biol Chem. 2007; 282:12687–97. [PubMed: 17339321]
28. Sokolov S, Kraus RL, Scheuer T, Catterall WA. Inhibition of sodium channel gating by trapping the domain II voltage sensor with protoxin II. Mol Pharmacol. 2008; 73:1020–8. [PubMed: 18156314]
29. Cahalan MD. Modification of sodium channel gating in frog myelinated nerve fibres by Centruroides sculpturatus scorpion venom. J Physiol. 1975; 244:511–34. [PubMed: 1079869]
30. Koppenhofer E, Schmidt H. Effect of scorpion venom on ionic currents of the node of Ranvier. II. Incomplete sodium inactivation. Pflugers Arch. 1968; 303:150–61. [PubMed: 5692853]
31. Rogers JC, Qu Y, Tanada TN, Scheuer T, Catterall WA. Molecular determinants of high affinity binding of alpha-scorpion toxin and sea anemone toxin in the S3-S4 extracellular loop in domain IV of the Na+ channel alpha subunit. J Biol Chem. 1996; 271:15950–62. [PubMed: 8663157]
32. Cestele S, et al. Voltage sensor-trapping: enhanced activation of sodium channels by beta-scorpion toxin bound to the S3-S4 loop in domain II. Neuron. 1998; 21:919–31. [PubMed: 9808476]
33. Cestele S, et al. Structure and function of the voltage sensor of sodium channels probed by a beta-scorpion toxin. J Biol Chem. 2006; 281:21332–44. [PubMed: 16679310]
34. Cohen L, et al. Direct evidence that receptor site-4 of sodium channel gating modifiers is not dipped in the phospholipid bilayer of neuronal membranes. J Biol Chem. 2006; 281:20673–9. [PubMed: 16720570]
35. Tejedor FJ, Catterall WA. Site of covalent attachment of alpha-scorpion toxin derivatives in domain I of the sodium channel alpha subunit. Proc Natl Acad Sci U S A. 1988; 85:8742–6. [PubMed: 2847174]
36. Marcotte P, Chen LQ, Kallen RG, Chahine M. Effects of Tityus serrulatus scorpion toxin gamma on voltage-gated Na+ channels. Circ Res. 1997; 80:363–9. [PubMed: 9048656]
37. Campos FV, Chanda B, Beirao PS, Bezanilla F. beta-Scorpion toxin modifies gating transitions in all four voltage sensors of the sodium channel. J Gen Physiol. 2007; 130:257–68. [PubMed: 17698594]
38. Campos FV, Chanda B, Beirao PS, Bezanilla F. Alpha-scorpion toxin impairs a conformational change that leads to fast inactivation of muscle sodium channels. J Gen Physiol. 2008; 132:251–63. [PubMed: 18663133]

39. Cha A, Ruben PC, George AL Jr. Fujimoto E, Bezanilla F. Voltage sensors in domains III and IV, but not I and II, are immobilized by Na+ channel fast inactivation. Neuron. 1999; 22:73–87. [PubMed: 10027291]
40. Sheets MF, Kyle JW, Hanck DA. The role of the putative inactivation lid in sodium channel gating current immobilization. J Gen Physiol. 2000; 115:609–20. [PubMed: 10779318]
41. Banerjee A, MacKinnon R. Inferred motions of the S3a helix during voltage-dependent K+ channel gating. J Mol Biol. 2008; 381:569–80. [PubMed: 18632115]
42. Ruta V, Jiang Y, Lee A, Chen J, MacKinnon R. Functional analysis of an archaebacterial voltage-dependent K+ channel. Nature. 2003; 422:180–5. [PubMed: 12629550]
43. Herrington J, et al. Blockers of the delayed-rectifier potassium current in pancreatic beta-cells enhance glucose-dependent insulin secretion. Diabetes. 2006; 55:1034–42. [PubMed: 16567526]
44. Lee CW, et al. Solution structure and functional characterization of SGTx1, a modifier of Kv2.1 channel gating. Biochemistry. 2004; 43:890–7. [PubMed: 14744131]
45. Armstrong CM. Na channel inactivation from open and closed states. Proc Natl Acad Sci U S A. 2006; 103:17991–6. [PubMed: 17101981]
46. Chanda B, Asamoah OK, Bezanilla F. Coupling interactions between voltage sensors of the sodium channel as revealed by site-specific measurements. J Gen Physiol. 2004; 123:217–30. [PubMed: 14981134]
47. Wan X, Chen S, Sadeghpour A, Wang Q, Kirsch GE. Accelerated inactivation in a mutant Na(+) channel associated with idiopathic ventricular fibrillation. Am J Physiol Heart Circ Physiol. 2001; 280:H354–60. [PubMed: 11123251]
48. Bennett PB, Yazawa K, Makita N, George AL Jr. Molecular mechanism for an inherited cardiac arrhythmia. Nature. 1995; 376:683–5. [PubMed: 7651517]
49. Spampanato J, Escayg A, Meisler MH, Goldin AL. Generalized epilepsy with febrile seizures plus type 2 mutation W1204R alters voltage-dependent gating of Na(v)1.1 sodium channels. Neuroscience. 2003; 116:37–48. [PubMed: 12535936]
50. Bendahhou S, Cummins TR, Tawil R, Waxman SG, Ptacek LJ. Activation and inactivation of the voltage-gated sodium channel: role of segment S5 revealed by a novel hyperkalaemic periodic paralysis mutation. J Neurosci. 1999; 19:4762–71. [PubMed: 10366610]

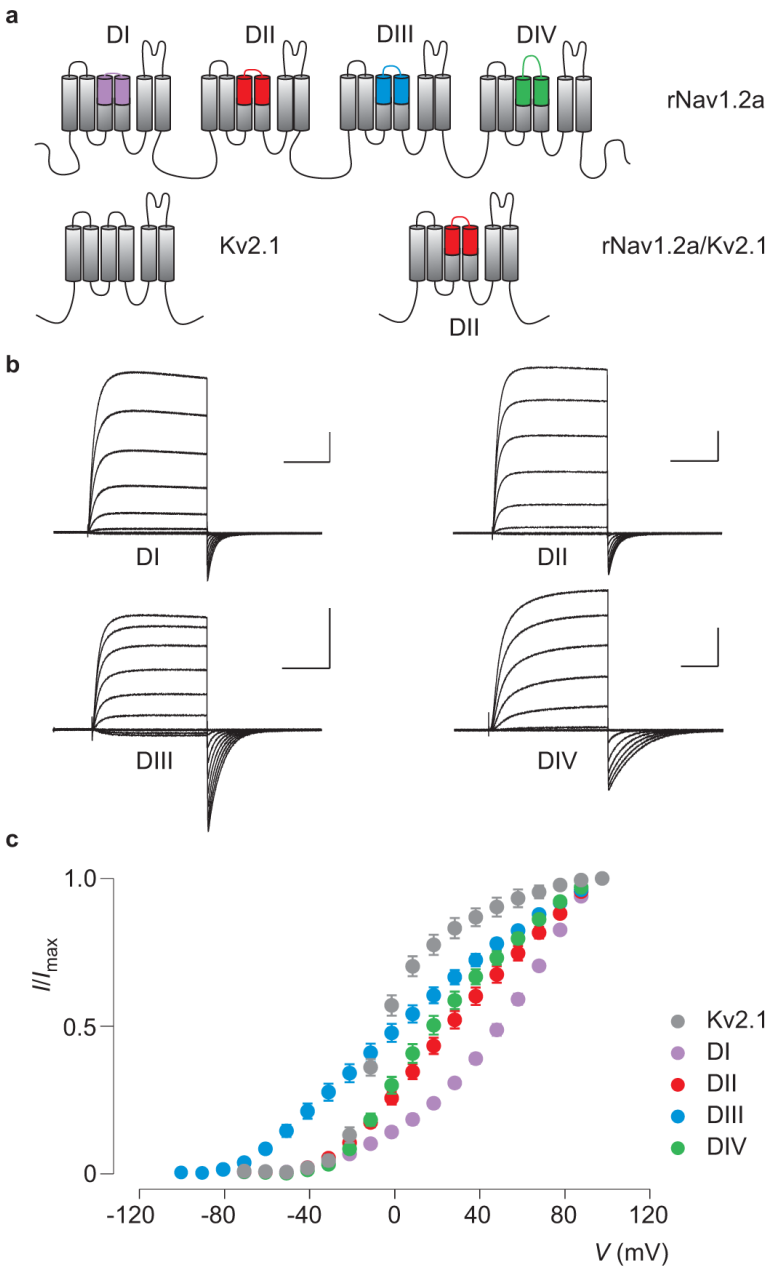

Figure 1. Transfer of the voltage sensor paddle motifs from rNav1.2a to Kv2.1

a, Cartoon depicting the paddle motif transfer from the Nav channel S1-S4 voltage sensor of domain II into Kv2.1. Purple: domain I paddle (DI), red: domain II paddle (DII), blue: domain III paddle (DIII) and green: domain IV paddle (DIV). Color code will be used in all figures. **b,c,** Families of potassium currents (b) and tail current voltage-activation relationships (c) for each chimaera (n = 18, error bars represent s.e.m.). Holding voltage was -90mV and the tail voltage was -50mV (-80mV for DIII). Scale bars in (b) are 2 μA and 100 ms.

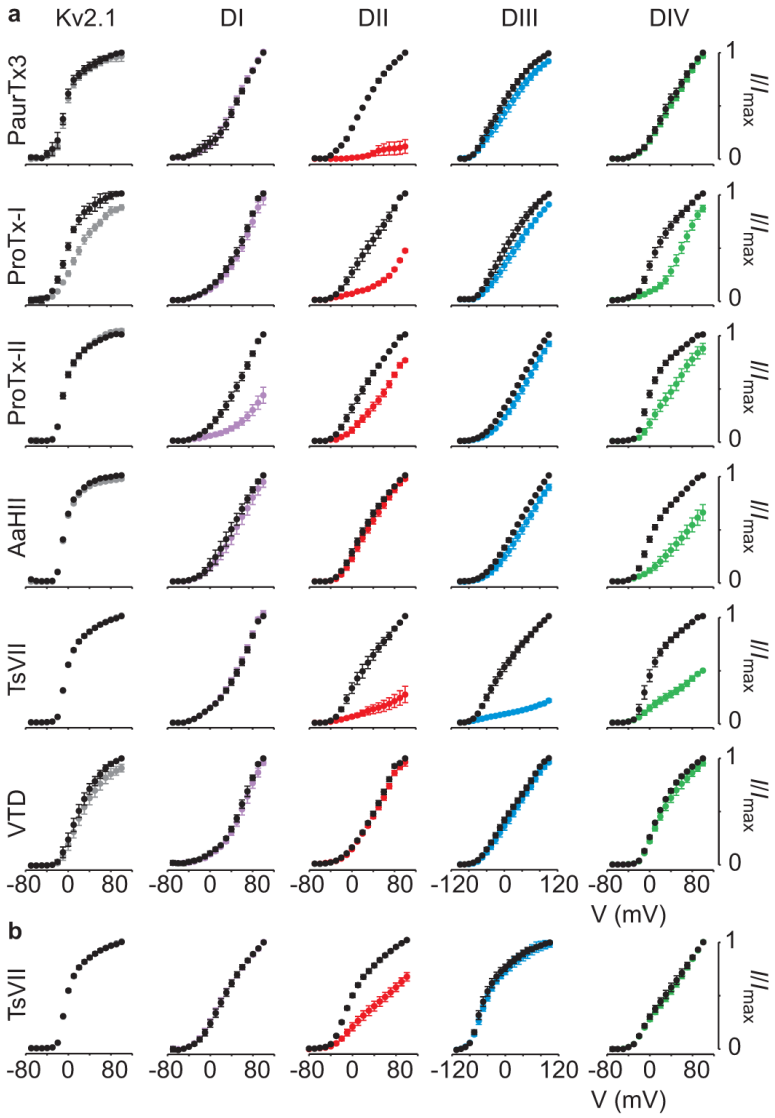

Figure 2. Sensitivity of rNav1.2a paddle chimaeras to extracellular toxins

a, Effects of toxins on Kv2.1 and chimaeras where paddle motifs were transferred from rNav1.2a into Kv2.1. Normalized tail current voltage-activation relationships are shown where tail current amplitude is plotted against test voltage before (black) and in the presence of toxins (other colors). Data are grouped per toxin (horizontally) and per chimaera or wild-type Kv2.1 (vertically). Concentrations used are 100nM PaurTx3, ProTx-I and ProTx-II; 1μM AaHII; 500nM TsVII and 100μM VTD. **b,** Effects of TsVII (50 nM) on rNav1.4 paddle chimaeras. n = 3-5 and error bars represent s.e.m. The plant alkaloid veratridine (VTD) is used as a negative control. The holding voltage was -90mV, test pulse duration was 300 ms, and the tail voltage was -50mV (-80mV for DIII).

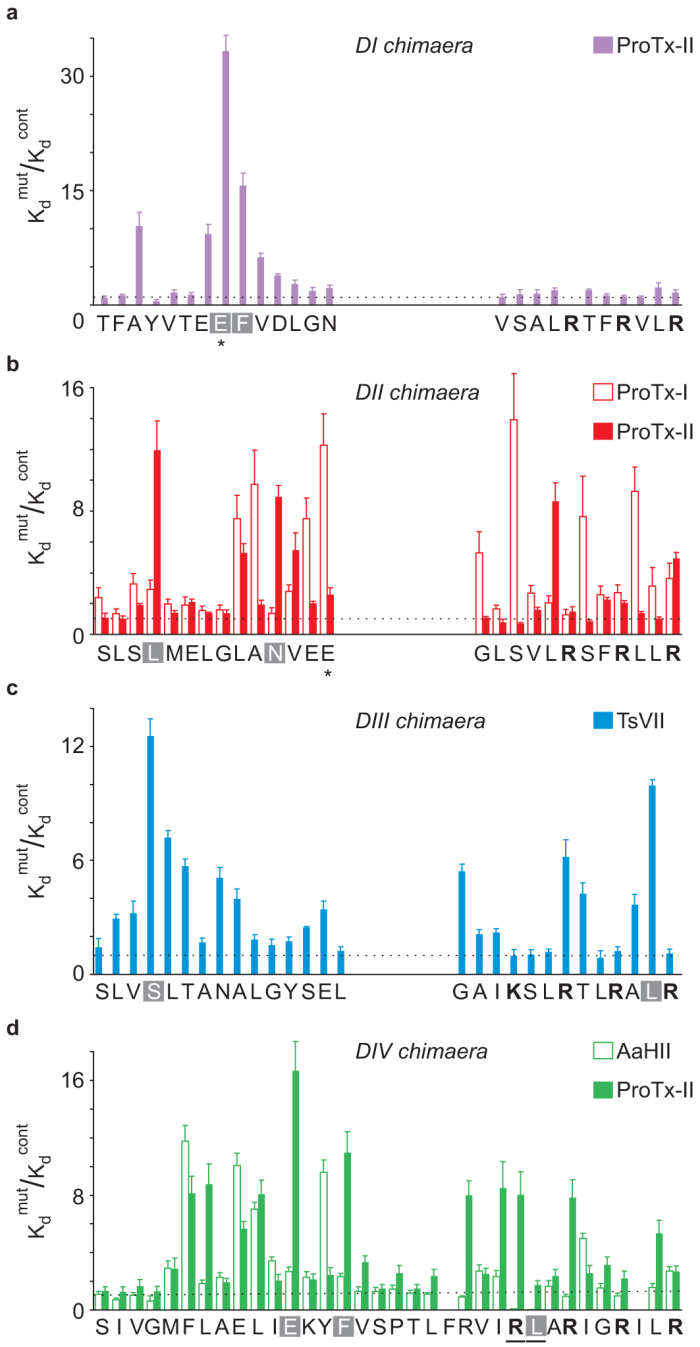

Figure 3. Scanning mutagenesis of Nav channel paddle motifs

a-d, Ala-scan of the separate rNav1.2a paddle motifs in the DI to DIV chimaeras where changes in apparent toxin affinity (K_d^{mut}/K_d^{cont}) are plotted for individual mutants. See Full Methods, Supplementary Fig. 4, 5c and Supplementary Table 3 for information on K_d measurements. Most of the residues within the rNav1.2a paddle in the four chimaera constructs were individually mutated to Ala (except for native Ala residues, which were mutated to Val). The dashed line marks a value of 1. Each mutant was initially examined using a concentration near the K_d value determined for the control chimaera (see

Supplementary Fig. 4). Mutants with a K_d^{mut}/K_d^{cont} value greater than five were further examined using a wider range of concentrations. Glu residues marked with asterisks were also mutated to a Lys. Bar diagrams are approximately aligned according to the sequence alignment of the different paddles (see Supplementary Fig. 1). Mutants without a corresponding bar did not result in functional channels. Residues with a grey background were used in subsequent tests (Fig. 4). Mutation of two underlined residues in (d) results in an increase in AaHII affinity (K_d = 235 ± 24nM for R1629A, 205 ± 23nM for L1630A and 1902 ± 102nM for the DIV chimera). n = 3-5 for each toxin concentration and error bars represent s.e.m.

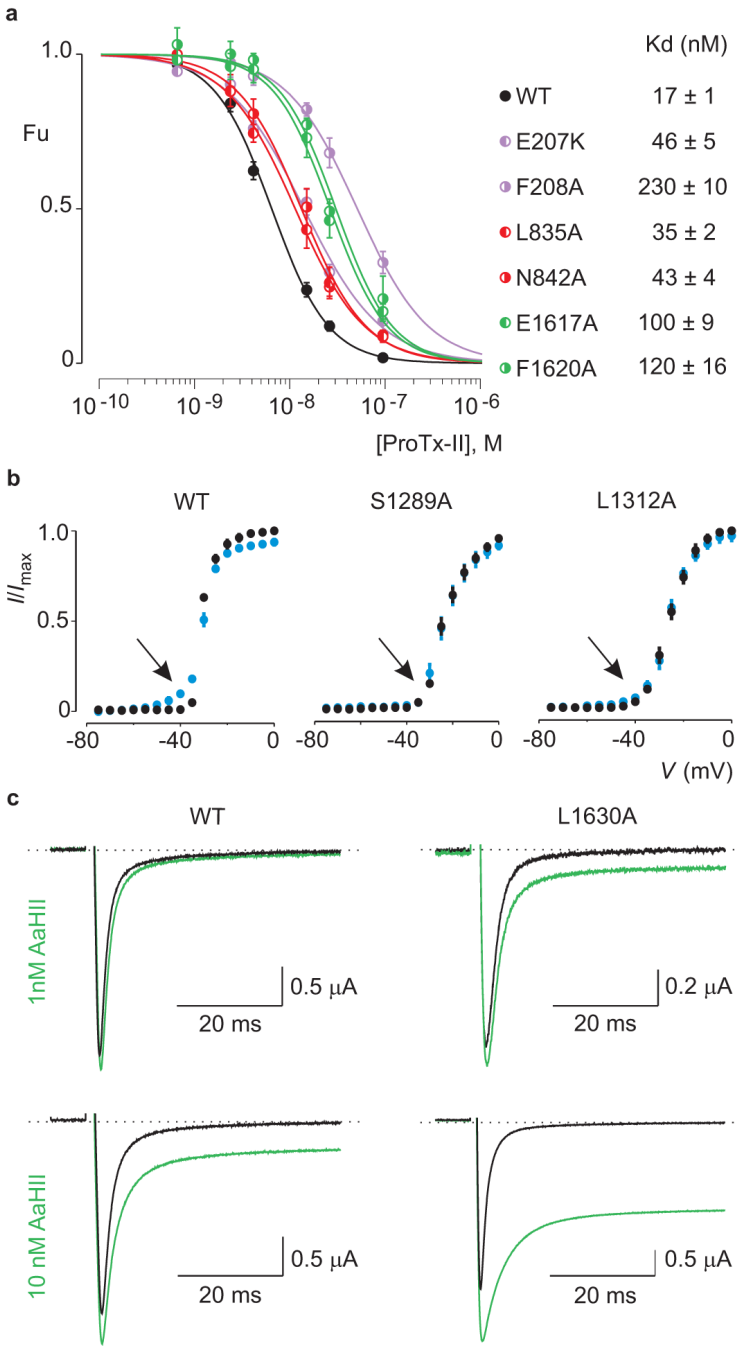

Figure 4. Reconstitution of paddle mutants into rNav1.2a and their effects on toxin-channel interactions

a, Concentration-dependence for ProTx-II inhibition of rNav1.2a and selected mutants plotted as fraction unbound (Fu) measured at negative voltages. Solid lines are fits of the Hill equation to the data with apparent K_d values shown. See Supplementary Fig. 5b and Supplementary Table 3 for further information. **b,** Normalized conductance-voltage relationships for rNav1.2a and two DIII mutants before and after addition of 50nM TsVII. Arrow indicates toxin effect or lack thereof. Holding voltage was -90 mV. **c,** rNav1.2a

mutation L1630A increases affinity for AaHII. Sodium currents were elicited by a depolarization to -15 mV from a holding voltage of -90 mV. Green trace is after AaHII addition.

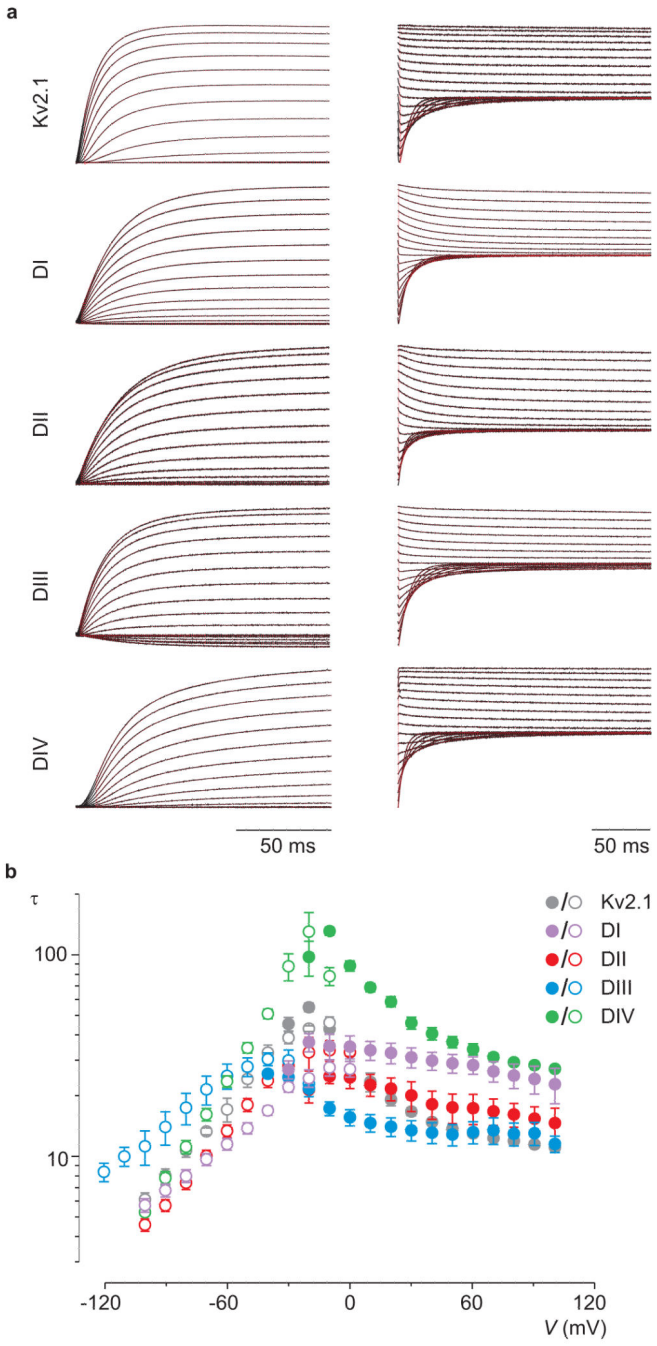

Figure 5. Kinetics of opening and closing for rNav1.2a/Kv2.1 chimaeras

a, Representative macroscopic currents (black) showing channel activation (left) and channel deactivation (right) using the following voltage protocols: activation, 10 mV incrementing steps to voltages between -40mV and +100mV from a holding potential of -90 mV; deactivation, 10 mV incrementing steps to voltages between 0mV and -100mV (-120mV for DIII) from a test voltage of between +80 and +100 mV (holding potential is -90 mV). Superimposed red curves are single exponential fits to the current records after initial lags in current activation. **b,** Mean time constants (τ) from single exponential fits to

channel activation (filled circles) and deactivation (open circles) plotted as a function of the voltage at which the current was recorded. n = 4-8 and error bars represent s.e.m.

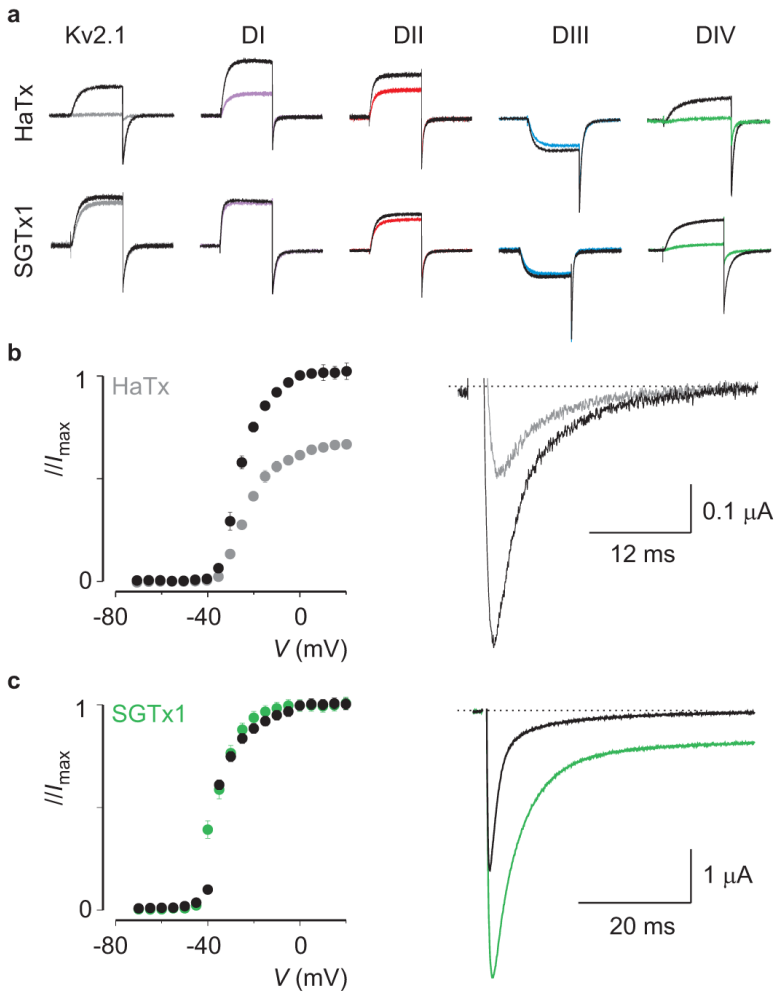

Figure 6. Identifying a tarantula toxin selective for the paddle motif in domain IV

a, Potassium currents elicited by depolarizations near the foot of the voltage-activation curve for Kv2.1 and chimaeras in the absence and presence of 50nM HaTx or 100nM SGTx1. The holding voltage was -90mV, test pulse duration was 300 ms, and the tail voltage was -50mV (-80mV for DIII). **b,** Conductance-voltage relationships for rNav1.2a before and after addition of 50nM HaTx (left), normalized to the maximal conductance in control. Sodium current elicited by a depolarization to -30 mV before and after addition of 50nM HaTx (right). **c,** Conductance-voltage relationship of rNav1.2a before and after addition of 100nM SGTx1 (left), individually normalized to the maximal conductance in either control or the presence of toxin. Sodium current elicited by a depolarization to -15 mV before and after addition of 100nM SGTx1 (right). n = 3-5 for each toxin concentration and error bars represent s.e.m (b, c).